Original

REPORT DOCUMENTATION PAGE

Form Approved
OMB NO. 0704-0188

1. AGENCY USE ONLY (Leave Blank)	2. REPORT DATE 6/1/2001	3. REPORT TYPE AND DATES COVERED Final Report, ~~03/01/1998 – 2/28/2001~~ Mar 02 98 Mar 01 01

4. TITLE AND SUBTITLE

Research on Algorithms and Performance in
Bayesian Automated Target Recognition

5. FUNDING NUMBERS
DAAG55-98-1-0102

2001 JUN 27 AM 10: 08

6. AUTHOR(S)

Anuj Srivastava and Jayaram Sethuraman

7. PERFORMING ORGANIZATION NAME(S) AND ADDRESS(ES)

Department of Statistics, Florida State University, Tallahassee, FL 32306

8. PERFORMING ORGANIZATION REPORT NUMBER

9. SPONSORING / MONITORING AGENCY NAME(S) AND ADDRESS(ES)

U. S. Army Research Office
P.O. Box 12211
Research Triangle Park, NC 27709-2211

RECEIVED
JUN 27 2001
BY

10. SPONSORING / MONITORING AGENCY REPORT NUMBER

38110.10-MA-RIP

11. SUPPLEMENTARY NOTES
The views, opinions and/or findings contained in this report are those of the author(s) and should not be construed as an official Department of the Army position, policy or decision, unless so designated by other documentation.

12 a. DISTRIBUTION / AVAILABILITY STATEMENT Approved for public release; distribution unlimited.	12 b. DISTRIBUTION CODE

13. ABSTRACT (Maximum 200 words)

The research reported here involves Bayesian ATR: development of statistical models and algorithms for statistical inference. The specific items that were covered are:

(i) Statistical Models for Thermal Variation in Prediction of IR Images: We are interested in statistical tools for predicting IR images of a known target in a new, previously unobserved thermal state. This prediction is based on a partial observation of the new state and the database of previous observation. We have developed a linear regression framework for estimating the temperature field, associated with the new state, and using it for predicting IR images from arbitrary perspectives.

(ii) Statistical Models for Clutter: We have derived analytical forms, called Bessel forms, to model the marginal densities of the filtered images, filtered using a set of Gabor filters. These analytical forms are easy to compute and match well with the observed histograms. In addition, a closed-form expression for the L^2 metric, on the space of these densities, provides a measure of closeness between natural images, with applications in clutter classification.

(iii) Nonlinear filtering for Tracking of Manifold-Valued Parameters: In ATR and other signal/image processing applications, we are often interested in tracking parameters that are constrained to be manifold-valued. We have applied a sequential Monte Carlo algorithm to solve the nonlinear, non-Euclidean filtering problem on these manifolds.

(iv) Asymptotic Performance Analysis: Bayesian ATR corresponds to selection of hypothesis in the presence of nuisance variables. Using Laplace's approximation to integrate out the nuisance variables (pose, location, motion etc.), we have derived analytical forms for the probabilities of error in ATR. Additionally, we have quantified the relation between nuisance estimation errors and the ATR performance.

14. SUBJECT TERMS Bayesian ATR, clutter model, nonlinear filtering, face tracking, principal subspace tracking	15. NUMBER OF PAGES 19
	16. PRICE CODE

17. SECURITY CLASSIFICATION OR REPORT UNCLASSIFIED	18. SECURITY CLASSIFICATION ON THIS PAGE UNCLASSIFIED	19. SECURITY CLASSIFICATION OF ABSTRACT UNCLASSIFIED	20. LIMITATION OF ABSTRACT UL

Acquisition of Equipment for Research in Bayesian Automated Target Recognition
Final Report
Grant Period: March 1, 1998 to February 28, 2001

Anuj Srivastava
Department of Statistics,
Florida State University,
Tallahassee, FL 32306

J. Sethuraman
Department of Statistics,
Florida State University,
Tallahassee, FL 32306

Contents

1 Statement of the Problem Studied

The equipment acquired under this DURIP grant is aimed for research in statistical automated target recognition (ATR) using remotely sensed images. We have focused on the problem of recognizing (known) targets from their infrared and video images. In addition to the variability associated with targets, their pose, motion, and thermal profiles, the targets are assumed to be present in cluttered environments. Taking a statistical approach, our main goal was to derive efficient probability models (analytical wherever possible) for these sources of variability in the observed images. Having obtained such probability models, we have derived algorithms for inferences and also quantified the algorithmic performance for specific ATR situations. The key idea behind this research is to isolate and model different physical variables individually, and derive models/estimators for each one of them. These results will be utilized towards the theory of a general purpose ATR algorithm which continues to be our research focus.

In particular, our research focused on the following aspects of ATR:

1. **FLIR ATR**: Infrared images exhibit a large variability due to the varying thermal states of the targets. Modeling the thermal states as scalar temperature fields on the target surfaces, we have developed a regression framework for predicting arbitrary FLIR images of known targets in partially observed but otherwise unknown thermal states. This tool can be used for constructing/refining image database or directly for FLIR ATR.

2. **Clutter Modeling and Classification**: Modeling the clutter pixels remains the most challenging component of the statistical ATR. Targets of interest seldom occur alone in the scenes and the presence of other objects leads to confusing clutter. We have derived coarse, tractable probability models for these clutter pixels and have applied them to classifying the clutter-type for natural images.

3. **Bayesian Inferences for ATR**: Once we have the probability models, the next task is to derive algorithms for inferences under these models. Since the ATR representations take values on manifold-valued space, we need a theory of inferences on such parameter spaces. We have built upon the previous work [15] to develop algorithms for estimation/tracking of manifold-valued parameters for ATR. Specifically, we have derived a nonlinear filter for tracking stochastic processes on (finite dimensional) Lie groups and their quotient spaces.

4. **Performance Analysis of Bayesian ATR**: Any inference procedure should be accompanied by its performance specifications, and we have derived metrics for analyzing performance for the following ATR tasks: (i) estimation of nuisance parameters such as pose, location, thermal state etc., and (ii) selection of maximum a-posterior hypothesis (target type) in the presence of estimated nuisance parameters. Using asymptotic arguments we have related the performance in target recognition to the performance in pose estimation in an analytical form. [3, 5]

2 Summary of Scientific Progress and Accomplishments

Next we describe the obtained under these items.

2.1 Prediction of IR Images

A recent meeting of the ARO strategy meeting shortlisted a number of high-priority research areas. In the area of **knowledge base acquisition and refinement**, it was stated that "Some means

of (database) construction and refinement on the fly .. is required. Generation of relevant multiple viewpoints for retraining of ATR functionality ... is desired".

To pursue database updating and "rapid retraining", we have developed a framework for predicting IR images of a known target in a new thermal state. We assume a prior database (mostly incomplete in terms of the target's thermal states) of target profiles and some partial observation of a new thermal state. The goal is to utilize the new observation, along with the prior database, to generate estimates of IR images from all other angles, in order to update the database. In our approach, the thermal states of the target are represented via scalar temperature fields and the prediction task becomes that of estimating the unobserved parts of the field, using the observed parts and the past patterns. This estimation is performed using regression models for relating the temperature variables, at different points on the target's surface, across different thermal states. A linear regression model is applied and experiments have been conducted using a laboratory target and a hand-held IR camera. Shown in the upper-middle panel of Figure 1 is the target used in preliminary experiments; the upper-left panel shows its CAD model and the upper-right panel shows an example IR image. We have modeled IR images as Gaussian random fields: the mean field is
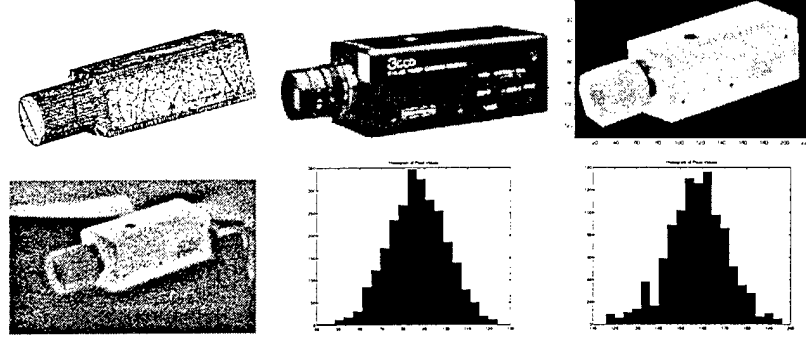

Figure 1: Top panels: CAD model (left), a video picture (middle), and an IR image (right) of the target used in experiments. Bottom panels: an IR image (left) and histograms (middle, right) of pixels in two homogeneous regions of that image.

given by the projection of 3D target temperature field onto the 2D image space. The histograms, in the bottom panels of Figure 1, display the pixel variations in two homogeneous regions of an IR image (bottom left panel), and hence, support the choice of a Gaussian model for the sensor noise.

Instead of storing past IR images, we propose organizing past database in form of scalar temperature fields, each associated with a distinct thermal state. Hence, **texture mapping** of IR images into (scalar) temperature fields becomes important. Observed IR images, of a target in a fixed thermal state, from multiple perspectives, are mapped using a (commercial) software onto the polygonal representation of its surface. Given this texture mapping, one can synthesize an IR image of this target in this thermal state, from an arbitrary perspective. Shown in the bottom panels (Figure 2) are some example images synthesized for a thermal state captured by six IR images (two of them are shown in the top panels). Using this procedure, we can generate a temperature field (via a texture map) for any previously observed thermal state of the target. Repeating this process for a number of thermal states, we obtain temperature fields for a number of previously observed thermal states; A principal component analysis of these fields result in a compact prior database of the thermal states, for use in prediction of IR images associated with the future thermal states.

Now consider the problem of estimating IR images, from multiple viewpoints, of a target in a partially observed thermal state. To setup the prediction experiment, the target was imaged in a
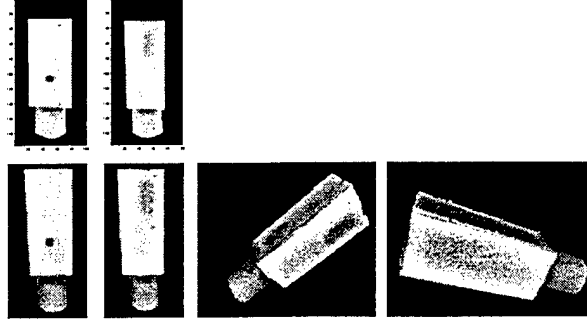
Figure 2: Texture mapping of IR images on the target surface to estimate the temperature field. Top panels: original IR images, bottom panels: synthesized IR images using texture maps.
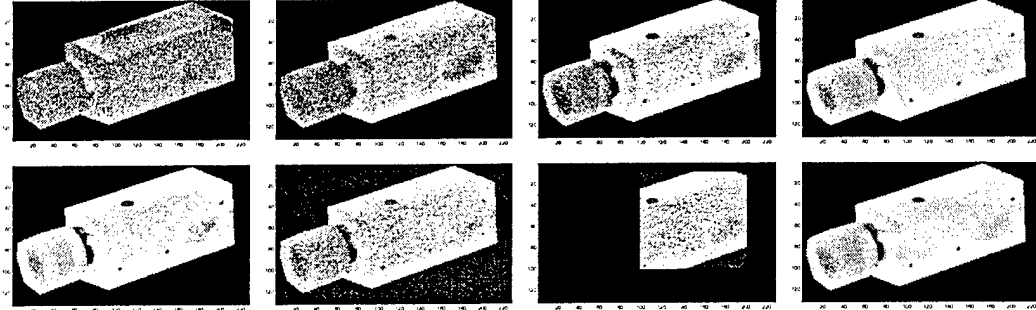

Figure 3: Upper panels: IR images of the target at prior thermal states, denoting the prior database Bottom panels: Estimation of an IR image using a noisy sub-image of the original.

new thermal state. In order to study the algorithmic performance, we have added white Gaussian noise (with a standard deviation of σ) to this image, in addition to the already existing sensor noise. We have simulated partial observations by selecting a sub-image from the original image and then using it in our regression algorithm to compute the remaining thermal field. Shown in the bottom left panel of Figure 3 is an image of the target in the true underlying thermal state and the same image with added white Gaussian noise is shown in bottom, second panel. The selected sub-image is shown in bottom, third panel and the estimated image is shown in bottom right. To analyze estimation performance, we compute the matrix 2-norm between the estimated and the original image (alternative performance metrics can be substituted instead). Let ρ denotes the fraction of the pixels selected in the sub-image, compared to the original image. Shown in Figure 4 is the plot of expected relative error versus σ, for $\rho = 1.12\%, 2.93\%, 9.21\%$, and 15.29%. As expected, the relative error decreases as ρ increases and the error increases with σ. If the estimated temperature field is found to be significantly different from the current database, it can be included in the database for database updating. This idea can also be used for database refinement, where a subset of the prior database is selected according to the current observations.

For details regarding this approach, please refer to the article [14]. This research is being performed in collaboration with Dr. Richard Sims of AMCOM and a graduate student, Brian Thomasson, of FSU.
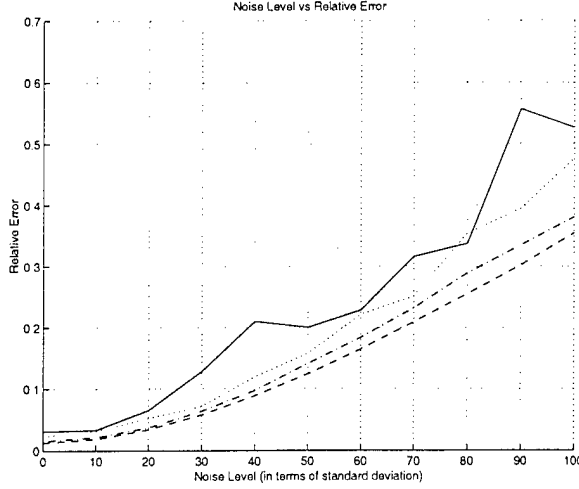
Figure 4: Variation of estimation error in IR image prediction versus the additive noise standard deviation in observed image, for four different values of ρ.

2.2 Clutter Modeling and Classification Metrics

Given an observed image of a target, imaged in a cluttered environment, one would like to characterize the clutter to the extent that it improves the ATR performance. Some knowledge of clutter type, whether it is grass, buildings, trees, or roads, can help improve the task of target recognition. We have derived coarse analytical models for representing image spectra and imposed L^2 metric on them to quantify image differences. An emerging approach, to representing and analyzing images, is to decompose them into their spectral bins, i.e. perform band-pass filtering of the images into different frequency bands, and then to study the statistics of these components. Studies (e.g. [1]) have shown that the human visual system also decomposes images into such frequency components. For implementation, these components are computed using linear filters, each tuned to a different frequency, scale and orientation; a formal framework for such spectral analysis was introduced in Gabor [2]. The marginal densities (histograms) of the components have often been chosen as the sufficient statistics, and have been successfully applied to modeling, analysis and even synthesis of homogeneous textures [7, 16, 6]. Let $F^{(j)}$, $j = 1, 2, \ldots, k$, be the linear filters that are used to decompose an image I into its spectral components. In this paper, we have utilized the Gabor filters although other such filters can also be used. We require that the filters be chosen such that the spectral components have marginal densities that are: (i) unimodal with a mode at zero, and (ii) symmetric around zero. Then, $I^{(j)} = I * F^{(j)}$ is a spectral component of the image I, where $*$ denotes the 2D convolution operation. We are interested in an analytical form that models the probability density of the pixels in $I^{(j)}$. Mathematically, an image pixel is modeled as

$$I(z) = \sum_i a_i g_i(z - z_i); z = [x \ y]^T, z_i = [x_i \ y_i]^T \ . \tag{1}$$

Here z is the variable for pixel location, g_i is a profile of a randomly chosen object, and a_i's are random weights associated with different profiles. a_i's are modeled as *i.i.d.* standard normal and the locations z_i's as modeled as samples from a 2D Poisson process, with a uniform intensity λ (independent of a_i's). Consider a pixel in the component $I^{(j)}$,

$$I^{(j)}(z) = \sum_i a_i g_i^{(j)}(z - z_i) \ , \quad \text{where} \quad g_i^{(j)} = F^{(j)} * g_i \ . \tag{2}$$

6

$I^{(j)}(z)$ is a random variable and we want to characterize its randomness. The conditional density of $I^{(j)}(z)$, given the Poisson points $\{z_i\}$ and the profiles $\{g_i\}$, is $N(0, u)$, where the random variable u is defined as the quantity $\sum_i (g_i^{(j)}(z - z_i))^2$.

For general cases, with completely unknown objects in the image, a broad family of distributions, not relying on a prior knowledge of the g_i's, is required. u has some distribution on the positive real line and, motivated by empirical studies, we model it by a scaled Γ-density: $f_u(u) = \frac{1}{c\Gamma(p)}(u/c)^{p-1}\exp(-u/c); p, c \in I\!\!R_+$, where p is called the *shape parameter* and c is called the *scale parameter* of u. Now we can integrate over the Poisson and profile variation, and derive the marginal density of $I^{(j)}(z)$. This density is given by:

Theorem 1 *Under the proposed model, the density function of $I^{(j)}(z)$ is: for $p > 0$ and $c > 0$,*

$$f(t; p, c) = \frac{1}{\sqrt{\pi}\Gamma(p)(2c)^{\frac{p}{2}+\frac{1}{4}}}|t|^{p-\frac{1}{2}}K_{p-\frac{1}{2}}(\sqrt{\frac{2}{c}}|t|) , \qquad (3)$$

where K is the modified Bessel function.

We call this structure of f as a *Bessel form*. Let $\mathcal{D}$ denote the set of all such Bessel forms: $\mathcal{D} = \{f(\cdot; p, c)|c, p \in I\!\!R_+\}$. As stated in [4], the shape parameter p provides some idea about the nature of the component $I^{(j)}$ (and hence about I). For $p = 1$, $f(t; 1, c)$ is the density of a double exponential or the *exponential model*. In general, $f(t; p, c)$ is the pth convolution power of the double exponential density. If $p > 1$, we call it *super-exponential model*, and we get closer to the Gaussian, especially if $p >> 1$. On the other hand, if $p < 1$, we call it *sub-exponential model*, the cusp of the density at zero becomes more pronounced.

How to estimate a Bessel form for a given spectral component $I^{(j)}$? Since the probability density f takes a parametric form, with parameters p and c, this task reduces to that of estimating p and c under an appropriate criterion. We have utilized a maximum-likelihood estimation (MLE) procedure to estimate p and c, according to:

$$\hat{p} = \frac{3}{\text{kurtosis}(I^{(j)}) - 3}, \quad \hat{c} = \frac{\text{variance}(I^{(j)})}{\hat{p}} , \qquad (4)$$

where variance and kurtosis are the sample variance and the sample kurtosis of the elements of $I^{(j)}$, respectively. We illustrate some estimation results for natural images.

- Shown in the top panels of Figure 5 are some real images taken from the Groningen database. The middle panels display their specific filtered forms (or the spectral components) for Gabor filters chosen at arbitrary orientations, and the bottom panels plot the marginal densities. On a log scale, the observed densities (histograms) are plotted in broken lines and the estimated Bessel forms ($f(x; \hat{p}, \hat{c})$) are plotted in solid lines.

- Shown in Figure 6 is another example. For the image shown in the top panel we have computed the observed and the estimated marginals for a number of Gabor filters. The middle panels plot the marginals for different filter orientations ($\theta = 30, 60, 90, 120$, and 150 degree) while keeping the scale fixed at $\sigma = 4.0$, and the bottom panels are for different filter scales ($\sigma = 1, 2, 3, 4$, and 5) keeping the orientation fixed at $\theta = 150$.

In our experiments, we have found a remarkable fit between the observed and the estimated marginals, for a large set of filtered natural images.

To quantify the distance between two Bessel forms, we have chosen the L^2-metric on $\mathcal{D}$. It is possible that other metrics, such as the Kullback-Leibler divergence or the L^1 metric, may be more
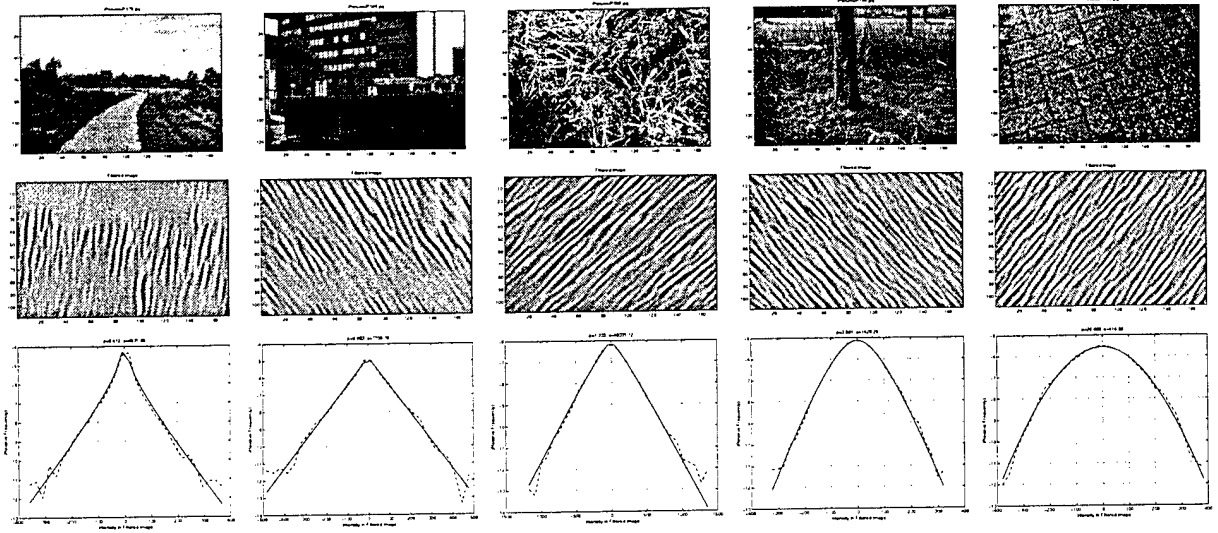
Figure 5: Images (top panels), their spectral components (middle panels), and the marginal densities (bottom panels). The observed densities are drawn in broken lines and the estimated Bessel forms are drawn in solid lines.

appropriate. L^2 is a common choice for search/optimization problems and also leads to a relatively simple expression. The main drawback of this choice is that the Bessel forms are not in L^2 for $p < 0.25$ and therefore the metric is not applicable to those cases.

Theorem 2 *The L^2-distance between the two Bessel densities, parameterized by (p_1, c_1) and (p_2, c_2), respectively, is given by: for $p_1, p_2 > 0.25$, $c_1, c_2 > 0$,*

$$d(p_1, c_1, p_2, c_2) = \left(\frac{1}{2\sqrt{2\pi}} \Gamma(0.5) \left(\frac{\mathcal{G}(2p_1)}{\sqrt{c_1}} + \frac{\mathcal{G}(2p_2)}{\sqrt{c_2}} - \frac{2\mathcal{G}(p_1 + p_2)}{\sqrt{c_1}} (\frac{c_1}{c_2})^{p_2} \mathcal{F} \right) \right)^{\frac{1}{2}}, \qquad (5)$$

where $\mathcal{G}(p) = \frac{\Gamma(p-0.5)}{\Gamma(p)}$ and $\mathcal{F} = F((p_1 + p_2 - 0.5), p_2; p_1 + p_2; 1 - \frac{c_1}{c_2})$ (F is the hypergeometric function).

Theorem 1 provides a metric between two Bessel forms, or between two spectral marginals. It can be extended to a metric on the image space as follows. For any two images, I_1 and I_2, and the filters $F^{(1)}, \ldots, F^{(K)}$, let the parameter values be given by: $(p_1^{(j)}, c_1^{(j)})$ and $(p_2^{(j)}, c_2^{(j)})$, respectively, for $j = 1, 2, \ldots, K$. Then, the L^2-distance, between the spectral representations of the two images, is defined as:

$$d_I(I_1, I_2) = \sqrt{\left(\sum_{j=1}^{K} d(p_1^{(j)}, c_1^{(j)}, p_2^{(j)}, c_2^{(j)})^2 \right)}. \qquad (6)$$

Consider the images of natural clutter shown in Figure 7. For a simple illustration, let the images in the top row be the training images that are already classified, and the bottom row be the images that are to be classified. Using nine small-scale Gabor filters ($K = 9$), for nine different orientations at a fixed scale, we have computed the pairwise distances d_I's. These distances are shown in the table below:
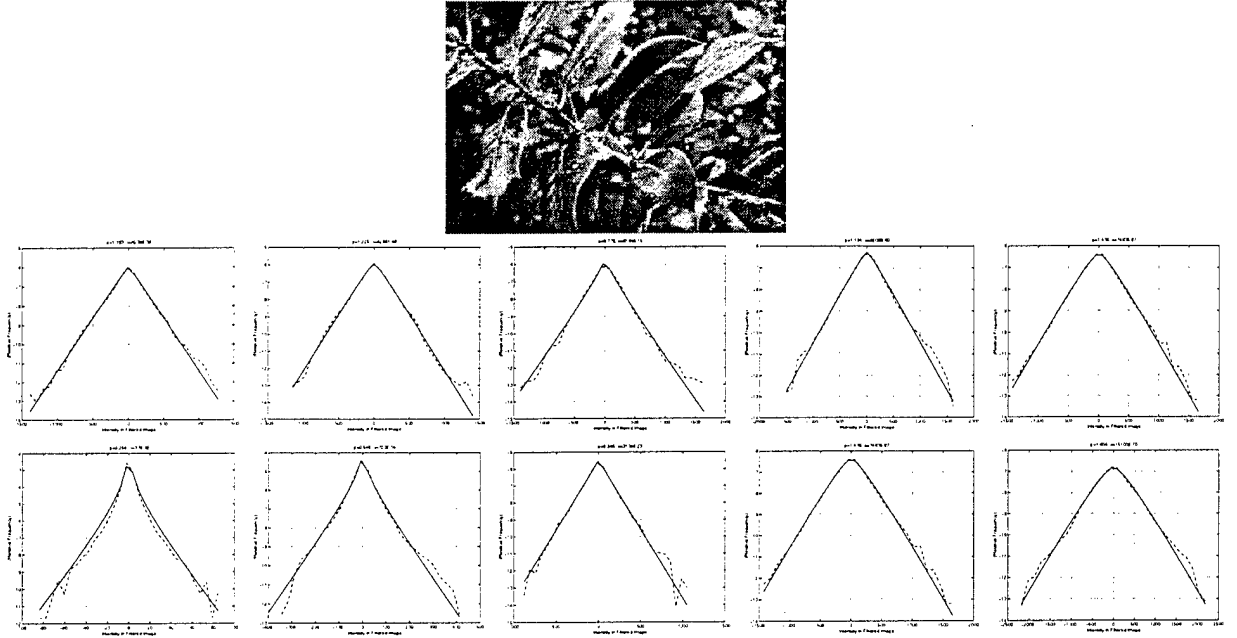
Figure 6: Plots of observed and estimated marginals (on a log scale) of the spectral components of a given image (top panel). Middle panels depict the marginals for different filter orientations: 30, 60, 90, 120, and 150, while the bottom panels are for different filter scales: 1, 2, 3, 4, and 5.

	I_1	I_2	I_3	I_4	I_5	I_6	I_7	I_8	I_9	I_{10}
I_1	0.00	0.51	0.61	0.63	0.59	0.64	0.85	0.92	0.74	0.70
I_2	0.51	0.00	0.59	0.61	0.60	0.65	0.86	0.93	0.71	0.67
I_3	0.61	0.59	0.00	0.46	0.69	0.72	0.89	0.96	0.67	0.62
I_4	0.63	0.61	0.46	0.00	0.71	0.74	0.90	0.97	0.63	0.57
I_5	0.59	0.60	0.69	0.71	0.00	0.48	0.81	0.89	0.78	0.76
I_6	0.64	0.65	0.72	0.74	0.48	0.00	0.78	0.87	0.81	0.78
I_7	0.85	0.86	0.89	0.90	0.81	0.78	0.00	0.76	0.94	0.92
I_8	0.92	0.93	0.96	0.97	0.89	0.87	0.76	0.00	0.99	0.98
I_9	0.74	0.71	0.67	0.63	0.78	0.81	0.94	0.99	0.00	0.48
I_{10}	0.70	0.67	0.62	0.57	0.76	0.78	0.92	0.98	0.48	0.00

Using the nearest neighbor approach, and the metric d_I listed in the table, we can correctly associate the test images with the corresponding training images. With a careful choice of filters, one can view d_I as a perception metric, i.e. a metric that seems to match well with our perception. To illustrate the classification of clutter types, we have plotted a clustering chart in the left panel of Figure 8 using the dendrogram function in matlab. This function generates a clustering tree for points in image space when their pairwise distances are given. The clustering of I_1 with I_2, I_3 with I_4, and so on, demonstrates the success of this representation and the metric chosen. For a quick comparison, a dendrogram clustering, using the Euclidean distances on the image space (i.e. $\|I_1 - I_2\|^2$, where $\| \cdot \|$ is the Frobenious norm), is shown in the right panel. Clearly, the Euclidean metric does not provide a satisfactory clustering. These results show that through Gabor filtering, the Bessel forms retain enough information to associate similar objects, to classify clutter type in cluttered ATR.

For details please refer to the articles [4, 12]. This research is being performed in collaboration with Prof. Xiuwen Liu of FSU and Prof. Ulf Grenander of Brown University.
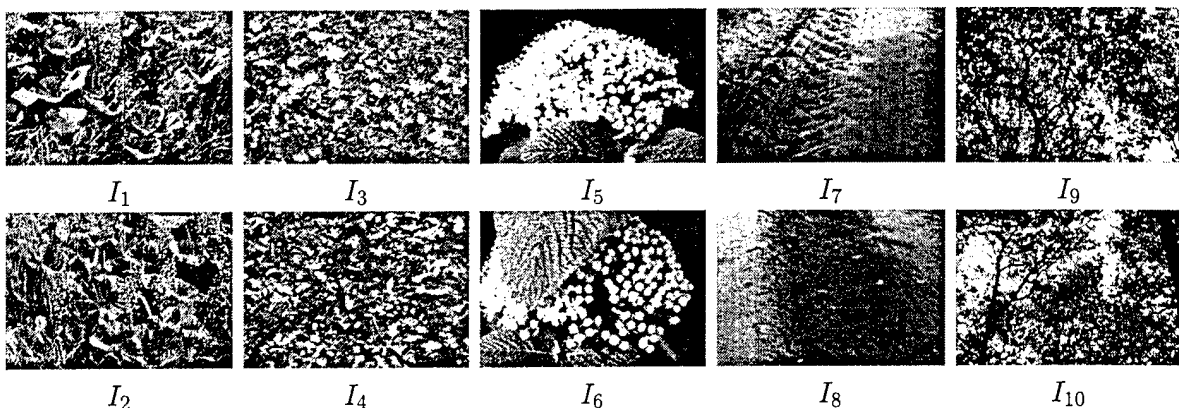
Figure 7: Ten natural images from the Groningen database: top row are the training images and bottom row are the test images.
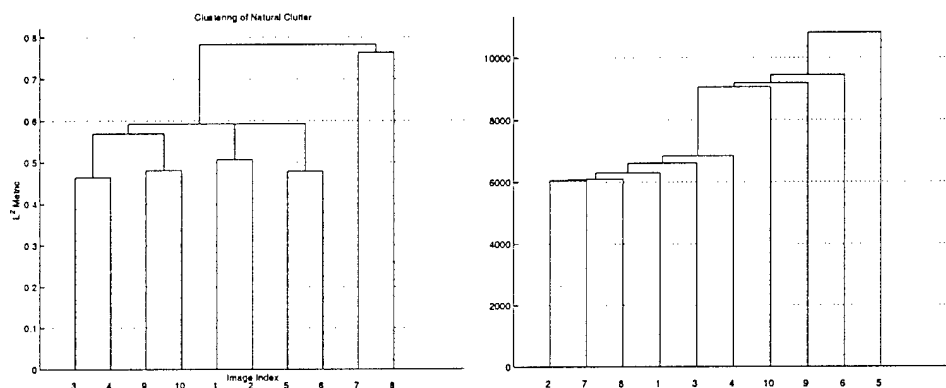

Figure 8: Dendrogram classification of images shown in Figure 7. Left panel: using image metric d_I, right panel: using Euclidean metric on image pixels.

2.3 Bayesian Filtering for Estimation/Tracking on Manifolds

In ATR and many other signal/image processing applications, the parameters of interest are often constrained to take values on manifolds. In this research, we have addressed the problem of tracking manifold-valued parameters using a nonlinear, non-Euclidean filtering approach. To establish a filtering framework, the system evolution is represented by trajectories on a manifold and a dynamics-based state equation is imposed on that space. This prior dynamic model combined with a likelihood function forms a time-varying posterior density on the manifold, to allow for Bayesian filtering and estimation. Using a sequential Monte Carlo method, or particle filtering, a recursive procedure is derived for propagating an estimate of this posterior (through random samples) in time. Posterior samples are then utilized to estimate the unknown parameters.

Let S be the manifold on which the parameter of interest lies: for rigid target tracking S is the Euclidean group of rigid motions, and for principal component tracking S is the Grassmann manifold. For discrete observation times $t = 1, 2, \ldots$, the system trajectory is given by the sequence $s_1, s_2, \ldots \in S$, and let the observation sequence be given by $Y_1, Y_2, \ldots$. Given the observation sequence $Y_{1:t} = \{Y_1, \ldots, Y_t\}$, the goal is to estimate the sequence $s_{1:t} = \{s_1, \ldots, s_t\} \in S^t$ using a minimum mean-squared error (MMSE) criterion. The nonlinear filtering equations are given by,

for $t = 2, 3, \ldots$

$$f(s_t|Y_{1:t-1}) = \int_S f(s_t|s_{t-1}) f(s_{t-1}|Y_{1:t-1}) \gamma(ds_{t-1}) , \tag{7}$$

$$f(s_t|Y_{1:t}) = \frac{f(Y_t|s_t) f(s_t|Y_{1:t-1})}{f(Y_t|Y_{1:t-1})} . \tag{8}$$

The filtering problem was studied for the following two applications:

1. **Face Tracking on Euclidean Group**: As an example of rigid tracking, we are interested in tracking of human faces from a video sequence. Using a deformable template approach, the target motion is tracked by tracking the rotations and translations (SE(3), special Euclidean group) that best match the synthesized images to the observed images. Shown in Figure 9 is an example of our face tracking software. One frame of the observed video sequence is shown in bottom right panel, and the 3D template of the face is rendered in top left. This template was generated using Minolta vivid700 3D scanner, and the scanned polygonated surface is shown in top-right panel. The likelihood function, used in the tracking, is proportional to the norm of the difference image between the observed and the hypothesized (an example is shown in bottom-left).
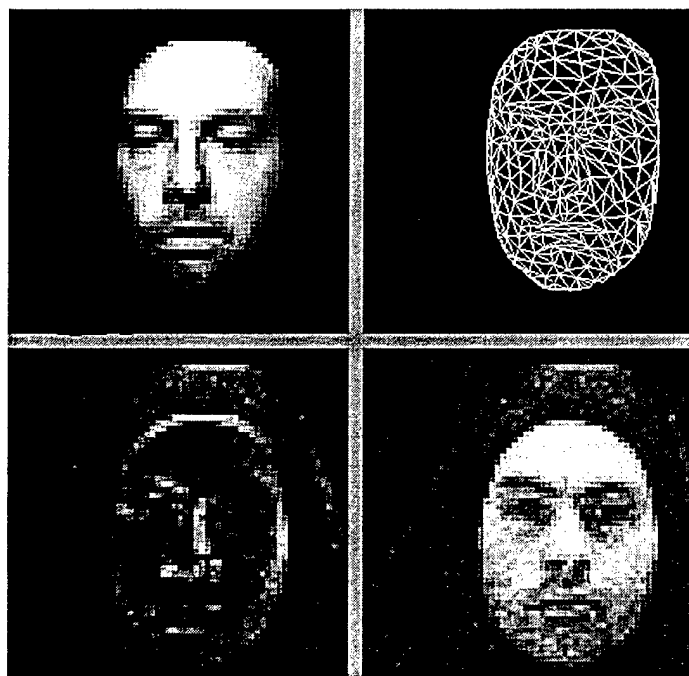

Figure 9: Illustration of face tracking: bottom-right is the video sequence for tracking, top-left is the rendering of out 3D face template, top-right is the polygonal surface of the template, bottom-left the difference image that provides a cost function for tracking.

This research is being performed in collaboration with Prof. Gordon Erlebacher of FSU and a graduate student Curt Hesher.

2. **Principal Component Tracking on Grassmann Manifold**: Consider the problem of principal subspace tracking in array signal processing, using a narrowband, uniform linear-array (ULA) consisting of n elements at half-wavelength spacing each. Furthermore, assume

that there are m signal transmitters, and the sensor output is modeled according to classical narrowband signal model [13]. The novel parts of this research are: (i) Posing the subspace tracking problem as that of inferences about trajectories on complex Grassmann manifold. (ii) Establishing the notion of geodesics and motion variables on Grassmannians, in order to impose dynamical models. This framework allows for learning the dynamical model from the past trajectories and use them for tracking future ones. (iii) Using a dynamic model, along with an observation model, to treat subspace tracking as a problem in nonlinear filtering. (iv) Application of a sequential Monte Carlo algorithm to approximate the time-varying posterior density on the Grassmannian. In addition to estimating MMSE subspaces, this sampling also allows for the estimation of expected errors and other posterior moments, for performance diagnostics. Together, these contributions lead to a fundamental and widely applicable algorithm for subspace tracking or, more generally, for tracking on quotient spaces of finite-dimensional Lie groups.

Figure 10 displays the tracking results for two datasets. Each plot shows the estimation error $\|s_t - \hat{s}_t\|$ for three different estimation procedures. First, the error associated with the instantaneous maximum-likelihood estimate (MLE), obtained by SVD of the instantaneous covariance matrix, is shown in the broken line. The error resulting from an adaptive procedure, relying on the SVD of a covariance matrix (using data over a sliding window) is shown in the dotted line. Finally, the estimation error for tracking from our method is plotted in bold.
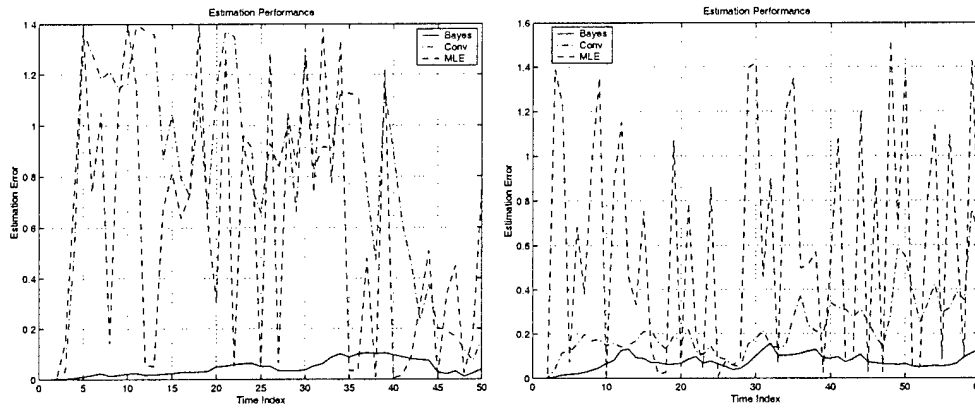

Figure 10: These panels plots the error in subspace tracking ($\|\hat{P}_t - P_t\|$) as a function of t for: (i) MLE (broken line), (ii) adaptive tracking (dotted line), and (iii) Bayesian tracking (solid line).

For details, please refer to the articles [9, 11, 10]. This research is being performed in collaboration with Prof. Eric Klassen of Department of Mathematics, FSU.

2.4 Asymptotic Bayesian ATR Performance Analysis

To recognize a target, estimation of the associated target attributes, such as pose, motion, lighting, and thermal profile, becomes essential. Target recognition is performed through Bayesian hypothesis testing; for a given observation the likelihood ratios are compared to the ratio of priors and a hypothesis is selected. In a binary case, for an observed image I, the Bayesian hypothesis-testing

problem is: $\frac{p(I|H_1)}{p(I|H_0)} \underset{H_0}{\overset{H_1}{\gtrless}} \frac{P(H_0)}{P(H_1)} \equiv \nu$. In the presence of nuisance parameters, such as pose and location, $p(I|H_i)$, $i = 0, 1$ is defined via the integral $p(I|H_i) = \int_S p(I|s, H_i)p(s|H_i)\gamma(ds)$, where s is a nuisance parameter. In most practical situations, the integrand is too complicated to be computed analytically. To obtain analytical expressions, which are often more attractive, asymptotic approximations using Laplace's method has been derived.

Lemma 1 *For any $\alpha \in \mathcal{A}$, a uniform prior (prior is given by Haar measure) and an asymptotic situation ($\sigma \to 0$), the likelihood function $p(I|\alpha)$ is given by*

$$\frac{1}{Z(\sigma)} \int_S \exp\{-\frac{1}{2\sigma^2}E(s,\sigma)\}\gamma(ds) \sim \frac{(2\pi)^{m/2}}{Z(\sigma)} \exp\{-\frac{1}{2\sigma^2}E(s^*,\sigma)\}\sqrt{\frac{(2\sigma^2)^m}{\det(\ddot{E}(s^*,\sigma))}}, \quad (9)$$

where $E = -\log(p(I|s,H)$, $s^* = \arg\min_{s\in S} E(s,\sigma)$ and $\ddot{E}$ is the Hessian of the function E with respect to s.

This approximation leads to an analytical form for the probability of error in binary target recognition.

Theorem 3 *Assuming the VIDEO sensor model with additive Gaussian noise, the probability of misclassification of the first kind (selecting H_1 when H_0 is true with parameter s_0) is given by $\frac{1}{\sqrt{2\pi}\kappa} \exp\left(-\kappa^2/2\right)$, where*

$$\kappa = \left(\beta\log(\nu) - \frac{\beta}{2}\log\frac{\det(\ddot{E}_{\alpha_0}(s_0,0))}{\det(\ddot{E}_{\alpha_1}(s_1,0))} + \frac{1}{2\beta} + R_{\alpha_1}(s_1) - R_{\alpha_0}(s_0)\right), \quad and \quad \beta = \frac{\sigma}{\sqrt{l_0^2 + l_1^2 - 2\rho}}.$$

Shown in Figure 11 are the plots for the probability of identifying *truck* when the actual target used in generating I was *tank*, using the VIDEO sensing model. For comparison, the experimental approximation of this error probability is plotted along with the analytical approximation of Theorem 1. At each noise level, the experimental probability is computed from multiple realizations of additive noise, performing nuisance integration on $S = SO(2)$ using trapezoidal method for each realization, and finding the relative frequency of incorrect decisions. The solid line plots the analytical expression and the broken line plots the experimental approximation. Shown in the other three panels are the sample VIDEO images of the tank at the noise levels given by $\beta = 0.01, 0.02$ and 0.1.

3 List of Equipment Acquired with this Grant

The following items were purchased through this DURIP funding.

1. One SGI Octane workstation.

2. One Toshiba laptop computer

3. One Canon Digital Camera

4. Three desktop Dell personal computers

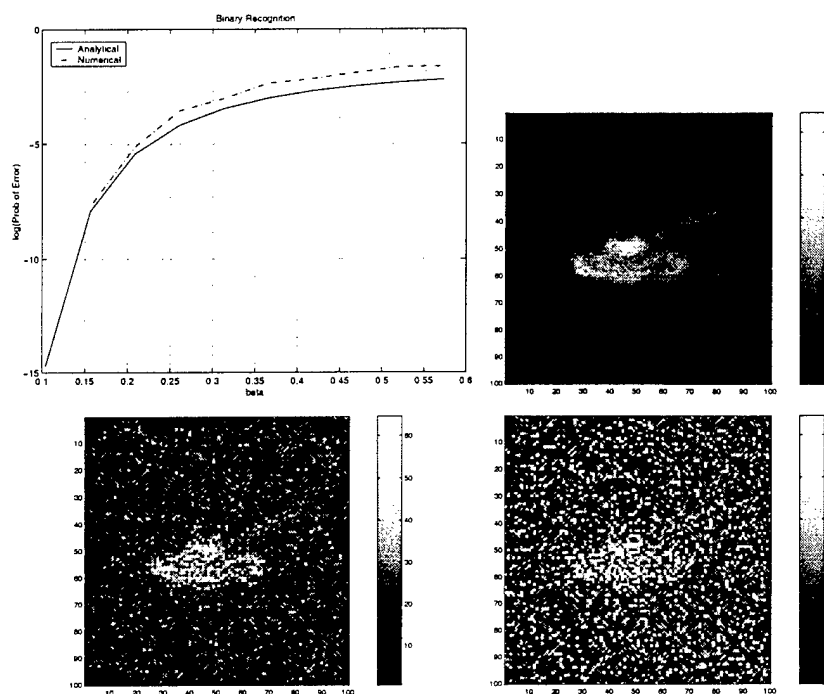5. One Gateway desktop personal computer

Figure 11: Top-left panel: the curves denote the log-probability of recognizing the truck when the tank is the true target (at certain pose), comparing the experimental results (broken line) with analytical estimates (solid line). The other three panels show VIDEO images of tank at noise levels given by $\beta = 0.01$ (top-right), 0.02 (bottom-left), and 0.1 (bottom-right).

6. Two Epson 800 inkjet printers

7. One HP b/w laser printer

8. One Panasonic TV/VCR combination.

9. Data cartridges, video tapes, computer cables, hard drives, SGI motherboard repair, SGI memory,

10. UPS power backup for SGI and other computers.

11. Splus and other statistical software.

12. Books and software manuals.

In addition to this DURIP award, we also received funding for acquiring equipment from NSF MRI award and the FSU Research Foundation. Combining this support, we have developed state of the art laboratory for research in image understanding. Named **Laboratory for Computational Vision**, it includes researchers from Statistics and Computer Science. Details about this laboratory can be obtained by visiting http://lcv.stat.fsu.edu. During this reporting period, our research has been benefited greatly from a number of imaging devices that were acquired for our Laboratory of Computational Vision. We have purchased two Minolta vivid700 three-dimensional scanners that can generate polygonal meshes (discretized surface) of the laboratory targets used in ATR experiments. These scanners have been used in generating CAD models for IR image prediction,

and for human face tracking from video sequences. We have also acquired a Raytheon PalmIR PRO thermal imager that operates in 7-14 μm spectral range and generates images of size 320 × 240 in 8-bit BMP format at a (typical) sensitivity level of 100mK. The scene temperature range for this camera, relative to the background, is 500°C. Additionally, we have also purchased two high-performance Olympus digital cameras, and a Sony digital video camera, that are being used in generating textures, natural images, and video sequences needed in several ongoing projects in the lab.

4 List of Publications

1. **List of Papers Published in Peer-Reviewed Journals**

   (a) Probability Models for Clutter in Natural Images, *IEEE Transactions of Pattern Analysis and Machine Intelligence*, vol 23, number 4, April 2001. (U. Grenander and A. Srivastava)

   (b) Asymptotic Performance Analysis of Bayesian Object Recognition, *IEEE Transactions on Information Theory*, vol 46, number 4, July 2000. (U. Grenander, A. Srivastava, and M. I. Miller).

   (c) A Bayesian Approach to Geometric Subspace Estimation, *IEEE Transactions on Signal Processing*, vol 48, number 5, May 2000. (A. Srivastava)

   (d) **Accepted for Publication**, Jump-Diffusion Markov Processes on Orthogonal Groups for Object Recognition, to appear in *Journal of Statistical Planning and Inference*. (A. Srivastava, G. Jensen, U. Grenander, and M. I. Miller).

   (e) Hilbert-Schmidt Bounds on Matrix Lie Groups for ATR, *IEEE Transactions on Pattern Analysis and Machine Intelligence*, vol 20, number 8, August 1998. (U. Grenander, M. I. Miller, and A. Srivastava)

2. **List of Papers Submitted to Peer-Reviewed Journals**

   (a) Analytical Probability Forms for Modeling Image Spectra, *IEEE Transactions on Pattern Analysis and Machine Intelligence*, submitted June 2001. (A. Srivastava, X. Liu, and U. Grenander)

   (b) Geometric Nonlinear Filtering for Subspace Tracking, in second review at *IEEE Transactions on Signal Processing*, June 2000. (A. Srivastava and E. Klassen)

   (c) Monte Carlo Extrinsic Estimators for Manifold-Valued Parameters, submitted to a special issue of *IEEE Transactions on Signal Processing*, December 2000. (A. Srivastava and E. Klassen)

3. **List of Papers Published as Book Chapters**

   (a) Bayesian Automated Target Recognition, *Handbook of Image and Video Processing*, Editor: Alan Bovik, Techbooks, Boston, 2000. (A. Srivastava, M. I. Miller and U. Grenander)

   (b) Monte-Carlo Techniques for Automated Target Recognition, *Sequential Monte Carlo Methods: Theory and Applications*, Editors: Gordon, Doucet, and DeFreitas, 2000. (A. Srivastava, A. Lanterman, U. Grenander, M. Loizeaux, and M. I. Miller).

4. **List of Papers Published in Non-Peer-Reviewed Journals/Conference Proceedings**
A. Srivastava

(a) A Compact Probability Model for Natural Clutter, *International Conference on Image Processing*, October 2001, Thessaloniki, Greece. (with U. Grenander)

(b) Analytical Models for Reduced Spectral Representations of Images, *International Conference on Image Processing*, October 2001, Thessaloniki, Greece. (with X. Liu and U. Grenander)

(c) A Regression Model for Prediction of IR Images, *SPIE Aerosense*, Orlando, FL, April 2001. (with B. Thomasson and S. R. F. Sims)

(d) Bayesian Filtering for Tracking Pose and Location of Rigid Targets, *SPIE Aerosense*, Orlando, FL, April 2000.

(e) Asymptotic Analysis of Pattern Theoretic Object Recognition, *SPIE Aerosense*, Orlando, FL, April 2000. (with M. Cooper).

(f) A Nonlinear Filtering Method for Geometric Subspace Tracking, *IEEE Sensor Array and Multichannel Processing workshop*, Boston, March 2000.

(g) Jump-Diffusion Processes on Matrix Lie Groups for Bayesian Inference, *IEEE Signal Processing workshop on Higher Order Statistics*, Caesaria, Israel, June 1999.

5. **List of Papers Presented at Meetings**
Anuj Srivastava:

(a) Geometric Tracking on Quotient Manifolds, *Annual meeting of Royal Statistical Society*, Scotland, UK, July 2001.

(b) Analytical Models for Spectral Analysis of Natural Images *Annual meeting of Royal Statistical Society*, Scotland, UK, July 2001.

(c) Nonlinear Filtering for Tracking Pincipal Subspaces, *AFOSR/AFRL workshop on Nonlinear Filtering*, Dayton, February, 2001.

(d) ATR via Pose and Location Estimation, *ARO CIS Annual Review Meeting*, Baltimore, March, 1999.

(e) Metrics for Recognizing Ground Targets, *AMCOM/ARO workshop on Metrics for ATR*, Huntsville, November, 1998.

(f) ATR Performance Analysis and Sensor Fusion, *ONR/GTRI workshop on Target Tracking and Sensor Fusion*, Atlanta, June, 1998.

Jayaram Sethuraman:

(a) Further properties of Dirichlet measures, presented at the 1998 *Luckacs Symposium "Statistics for the 21st Century"* at Bowling Green University, Bowling Green, April, 1998.

(b) Further properties of Dirichlet measures, presented at the *International Conference in Reliability and Survival Analysis* at Northern Illinois University, Dekalb, May, 1998.

(c) Specification of Joint Distributions from Marginal and Conditional Distributions, presented an invited paper at the *Symposium on Decision Theory* at Purdue University, Lafayette, June, 1998.

(d) Conformation in Metric pattern Theory, presented at the *Army Statistician's Conference* at New Mexico State University, Las Cruces, October, 1998.

(e) Conformation in Metric pattern Theory, presented at the meeting of the *Florida Chapter of the American Statistical Association* in Gainesville, February, 1999.

(f) Reduction in Predictive Ability Caused by Discretization of the Independent Variable – Presented at the *Army Statistics Conference* at West Point, October, 1999.

(g) Limit Theorems for Models in Pattern Analysis - Invited talk at the *International Conference on Stochastic Processes and their Applications* held at Cochin, India, December, 1999.

(h) Properties and Approximations of Dirichlet Processes at the *2000 Annual meeting of the Canadian Statistical Association* in Ottawa, ONT, June, 2000.

(i) Modeling Transmission Loss in a Large Network – presented at the *Army Conference on Applied Statistics* held at Rice University, Houston, October, 2000.

5   Scientific Personnel Supported

This DURIP funding was for acquisition of equipment and no personnel were support on this funding. Anuj Srivastava, Co-PI, and a graduate student Brian Thomasson are supported by a separate ARO grant DAAD19-99-1-0267.

6   Reports of Inventions

None.

References

[1] F. W. Campbell and J. G. Robson. Applications of fourier analysis to the visibility of gratings. *Journal of Physiology (London)*, 197:551–566, 1968.

[2] D. Gabor. Theory of communications. *Journal of IEE (London)*, 93:429–457, 1946.

[3] U. Grenander, M. I. Miller, and A. Srivastava. Hilbert-schmidt lower bounds for estimators on matrix lie groups for atr. *IEEE Transactions on PAMI*, 20(8):790–802, 1998.

[4] U. Grenander and A. Srivastava. Probability models for clutter in natural images. *IEEE Transactions on Pattern Analysis and Machine Intelligence*, 23(4), April 2001.

[5] U. Grenander, A. Srivastava, and M. I. Miller. Asymptotic performance analysis of bayesian object recognition. *IEEE Transactions of Information Theory*, 46(4):1658–1666, 2000.

[6] D. J. Heeger and J. R. Bergen. Pyramid-based texture analysis/synthesis. In *Proceedings of SIGGRAPHS*, pages 229–238, 1995.

[7] B. Julesz. A theory of preattentive texture discrimination based on first-order statistics of textons. *Biological Cybernetics*, 41:131–138, 1962.

[8] B. A. Olshausen and D. J. Field. Natural image statistics and efficient coding. *Network: Computation in Neural Systems*, 7, 1996.

[9] A. Srivastava. A bayesian approach to geometric subspace estimation. *IEEE Transactions on Signal Processing*, 48(5):1390–1400, 2000.

[10] A. Srivastava and E. Klassen. Monte carlo extrinsic estimators for manifold-valued parameters. *Special issue of IEEE Transactions on Signal Processing*, in review.

[11] A. Srivastava and E. Klassen. Geometric filtering for subspace tracking. *submitted to IEEE Transactions on Signal Processing*, June, 2000.

[12] A. Srivastava, X. Liu, and U. Grenander. Analytical probability forms for modeling image spectra. *IEEE Transactions on Pattern Analysis and Machine Intelligence*, in review, June, 2001.

[13] A. Srivastava, M. I. Miller, and U. Grenander. Multiple target direction of arrival tracking. *IEEE Transactions on Signal Processing*, 43(5):1282–85, May 1995.

[14] A. Srivastava, B. Thomasson, and S. R. F. Sims. A regression model of ir image prediction. *Proceedings of Aerosense: ATR XI*, 2001.

[15] Anuj Srivastava, Michael Miller, and Ulf Grenander. *Ergodic Algorithms on Special Euclidean Groups for ATR*. Systems and Control in the Twenty-First Century: Progress in Systems and Control, Volume 22. Birkhauser, 1997.

[16] S. C. Zhu, Y. N. Wu, and D. Mumford. "Minimax entropy principles and its application to texture modeling". *Neural Computation*, 9(8):1627–1660, November 1997.

A Publications and Research Monographs

Follwing published papers and the papers submitted to the journals are attached.

1. Probability Models for Clutter in Natural Images, *IEEE Transactions of Pattern Analysis and Machine Intelligence*, vol 23, number 4, April 2001. (U. Grenander and A. Srivastava)

2. Asymptotic Performance Analysis of Bayesian Object Recognition, *IEEE Transactions on Information Theory*, vol 46, number 4, July 2000. (U. Grenander, A. Srivastava, and M. I. Miller).

3. A Bayesian Approach to Geometric Subspace Estimation, *IEEE Transactions on Signal Processing*, vol 48, number 5, May 2000. (A. Srivastava)

4. Jump-Diffusion Markov Processes on Orthogonal Groups for Object Recognition, to appear in *Journal of Statistical Planning and Inference*. (A. Srivastava, G. Jensen, U. Grenander, and M. I. Miller).

5. Hilbert-Schmidt Bounds on Matrix Lie Groups for ATR, *IEEE Transactions on Pattern Analysis and Machine Intelligence*, vol 20, number 8, August 1998. (U. Grenander, M. I. Miller, and A. Srivastava)

6. Analytical Probability Forms for Modeling Image Spectra, *IEEE Transactions on Pattern Analysis and Machine Intelligence*, submitted June 2001. (A. Srivastava, X. Liu, and U. Grenander)

7. Geometric Nonlinear Filtering for Subspace Tracking, in second review at *IEEE Transactions on Signal Processing*, June 2000. (A. Srivastava and E. Klassen)

8. Monte Carlo Extrinsic Estimators for Manifold-Valued Parameters, submitted to a special issue of *IEEE Transactions on Signal Processing*, December 2000. (A. Srivastava and E. Klassen)

9. Bayesian Automated Target Recognition, *Handbook of Image and Video Processing*, Editor: Alan Bovik, Techbooks, Boston, 2000. (A. Srivastava, M. I. Miller and U. Grenander)